JOURNAL OF BACTERIOLOGY, Feb. 1975, p. 711-720

Vol. 121, No. 2
Printed in U.S.A.

Fruiting-Body Formation and Myxospore Differentiation and Germination in *Mxyococcus xanthus* Viewed by Scanning Electron Microscopy

L. SHIMKETS[1] AND T. W. SEALE*

Department of Biological Science, Florida State University, Tallahassee, Florida 32306

Received for publication 14 November 1974

Streaming cells, fruiting bodies, and single cells undergoing myxospore differentiation and germination were examined in the FB strain of *Myxococcus xanthus* by scanning electron microscopy. Myxospores differentiated in fruiting bodies differed in size, in kinetics of germination, in the fate of the myxospore capsule, and in the external structure of the walls of newly emerged cells when compared with myxospores differentiated in liquid medium after glycerol induction. Vegetative cells outgrowing from glycerol-induced myxospores were regularly pleomorphic, a condition that persisted through the first cell division.

Myxococcus xanthus is a flexible, gram-negative, rod-shaped bacterium that is unusual in the microbial world for a variety of morphological and physiological reasons. Three characteristics distinguish this organism from the eubacteria. First, vegetative cells possess the innate ability to aggregate into fruiting bodies and to form myxospores under conditions of nutritional stress. Second, the organism is motile by means of an enigmatic gliding mechanism. Third, it has the potential to lyse other bacteria and to utilize them as a source of nutrients.

Myxobacteria are attractive for ultrastructural, biochemical, and genetic analyses of developmental processes because these organisms possess the most complex life cycles found among prokaryotes. The differentiation of myxospores differs developmentally from endospore formation in *Bacillus* in that the entire vegetative cell becomes converted into a resting cell. A partial description of changes associated with myxospore formation and germination is available at the ultrastructural (1, 15, 17, 18, 19) and biochemical (2, 6, 9, 16, 20, 23) levels. Although speculations about the molecular bases for the control of these morphogenetic events have been presented (6, 9, 10, 21), the mechanisms by which these changes are regulated and effected remain both intriguing and unknown. Of further interest are the cell interaction and aggregation phenomena, which are necessary for fruiting-body formation. The general and varied importance of cell-cell interactions in the life style of myxobacteria, particularly *Myxococcus*, recently has been reviewed by Dworkin (7).

We used scanning electron microscopy to better visualize the following major features of the developmental cycle of *M. xanthus* schematically diagramed in Fig. 1: (i) coordinated cell streaming and the subsequent formation of the fruiting body; (ii) the process of myxospore differentiation; (iii) the process of myxospore germination; and (iv) the comparison of myxospores formed in fruiting bodies on solid medium and those formed in liquid medium after glycerol induction. The micrographs presented here provide an intimate view of the sequence of morphological changes that occur and complement and extend transmission electron microscopic (TEM) characterization of *Myxococcus* development by Voelz and Dworkin (18).

MATERIALS AND METHODS

Strains and cultural conditions. *M. xanthus* strain FB, obtained from M. Dworkin, was used throughout this study. This strain is useful because in liquid medium it is capable of growing in a dispersed manner. It easily can be induced to form myxospores. Cells were cultivated in 125-ml Erlenmeyer flasks containing 25 ml of liquid Casitone (Difco) medium and were incubated at 30 C in a reciprocating waterbath shaker at 92 strokes/min. The liquid medium was composed of 2% Casitone and 8×10^{-3} M $MgSO_4$ in distilled water.

Myxospore formation was induced by a modification of the glycerol method of Dworkin and Gibson (8). Sterile glycerol prewarmed to 30 C was added to mid-exponential-phase cells to a final concentration of 0.5 M, but in contrast to their method, we continued incubation in the same growth medium. Our medium omitted the 10^{-2} M PO_4 found in that of

[1] Present address: Department of Microbiology, University of Minnesota Medical School, Minneapolis, Minn. 55455.

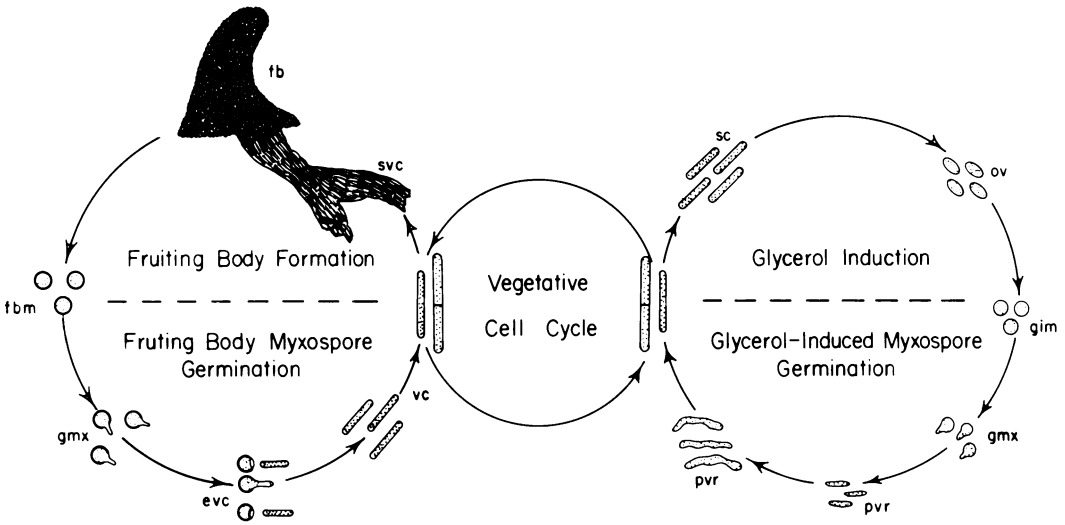

FIG. 1. *Life cycle of Myxococcus xanthus. Abbreviations: fb, Fruiting body; fbm, fruiting-body myxospores; gmx, germinating myxospore; evc, emerging vegetative cells; vc, vegetative cells; svc, swarming vegetative cells; sc, shortening vegetative cells; ov, ovoids; gim, glycerol-induced myxopores; pvr, pleomorphic vegetative rods.*

Dworkin and Gibson. Morphological changes were synchronous, and the population was converted to myxospores in 2 h. To effect germination, a population of myxospores induced by glycerol for 6 h was pelleted by centrifugation; the spores were immediately washed once in 0.1 M potassium phosphate buffer (pH 7.5) at 0 C and then suspended in an equivalent volume of fresh Casitone medium. The germination medium contained no added PO_4. When incubated as described above, germination and outgrowth were completed in 2 h.

Fixation and microscopy. To study fruiting-body formation, cells were streaked on medium containing 0.05% tryptone and 4% agar. Fruiting bodies appeared in 8 days. Agar slabs were sectioned from the plates and exposed to osmium vapors for 1 h (2% solution). The agar slabs were then ventilated overnight during which time the agar dried to hardness. Specimens were glued on aluminum stubs and coated as described below.

To examine the sequence of morphological changes during myxospore formation and germination, samples were removed from the cultures at various times, rapidly centrifuged to remove the medium, and then suspended in 0.05 M phosphate buffer (as above) containing 2% electron microscopic-grade glutaraldehyde (Polysciences, Inc.). Fixation was carried out for 2 h in an ice-water bath. After removal of the glutaraldehyde, cells were postfixed in 2% osmium tetroxide for 1 h in an ice-water bath. Cells then were washed once in phosphate buffer and three times in distilled water. The fixed and washed cell suspension was placed atop a glass cover slip and allowed to dry. Cover slips applied to aluminum scanning electron microscope stubs were coated with 20 nm of gold-palladium alloy (60:40) in a Denton DV-502 vacuum evaporator and were then examined in a Cambridge S4 Stereoscan scanning electron microscope. The accelerating voltage was 30 kV unless otherwise indicated.

RESULTS

The fruiting body of *M. xanthus* is a large aggregate of vegetative cells that have encysted to form myxospores; as such it represents the least complicated fruiting structure made by the myxobacteria. This structure is not simply derived from a colony but occurs when aggregation of vegetative cells at foci for fruiting results in their elevation from the substrate and conversion to myxospores. Figures 2 through 7 depict fruiting-body formation and structure. After a period of swarming over the surface of an agar plate, vegetative cells migrated in a coordinated fashion toward centers of aggregation as shown in Fig. 2 and 3. The cells in such streams were regularly oriented with regard to one another. Regions of an agar surface previously covered with millions of cells rapidly became devoid of them upon the initiation of oriented streaming. It appeared as if fruiting-body formation commenced when pyramidal layering of cells occurred at centers of aggregation (not shown). A typical mature fruiting body is seen in Fig. 4. Note that it appears to be composed only of myxospores and that almost all cells in the vicinity of the aggregation center participated in its formation. Figures 5, 6, and 7 show the basal, mid, and apical regions of a single fruiting body at a higher magnification. Immediately at the base of the fruiting body on the

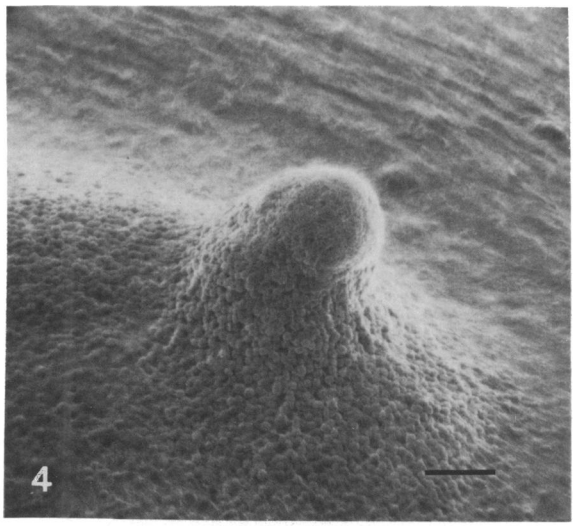

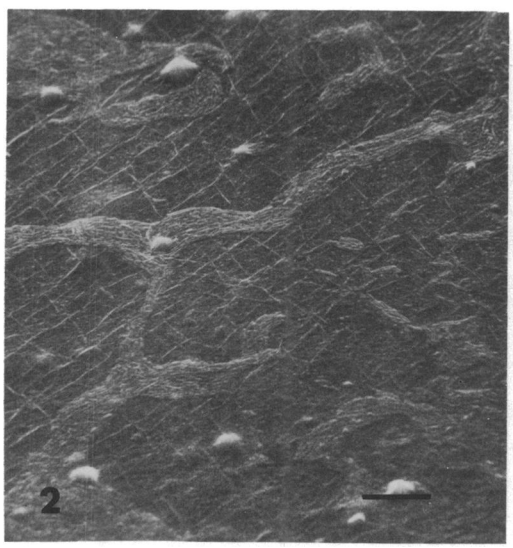

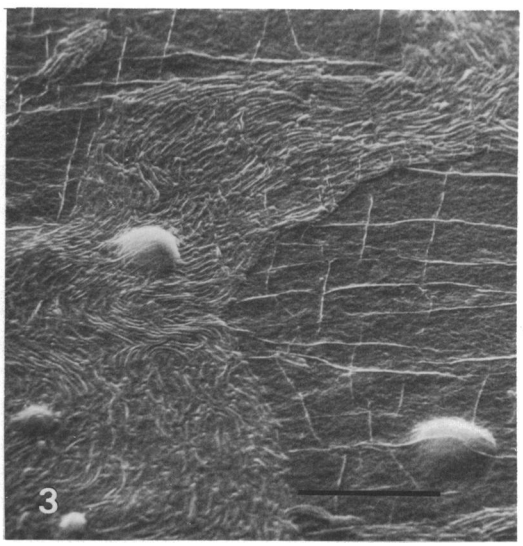

FIG. 2. *Aggregation and stream formation of M. xanthus vegetative cells upon initiation of fruiting-body formation. Scale marker is 10 μm. 55° tilt.*

FIG. 3. *Oriented gliding during aggregation of M. xanthus vegetative cells. Scale marker is 10 μm.*

FIG. 4. *Mature fruiting body of M. xanthus. Scale marker is 10 μm. 5 kV; 50° tilt.*

agar surface (Fig. 5) were degenerating vegetative cells that apparently were unable to undergo or to complete morphogenesis. Cells that had begun to shorten into myxospores can be seen at various stages as can scattered myxospores of different sizes. The cells were oriented rather uniformly, with their longitudinal axes directed toward the base of the fruiting body. The sheetlike slime matrix in which the mature, uniformly sized (about 2 μm) myxospores were embedded is shown in Fig. 6 and 7. Our preparations of fruiting bodies characteristically showed a thickened slime layer at their apexes (Fig. 7).

To better visualize the morphogenesis of myxospores from vegetative cells, we resorted to the glycerol induction method of Dworkin and Gibson (8). Myxospores were rapidly produced when 0.5 M glycerol was added to exponentially growing liquid cultures. Figures 8 through 12 show the sequence of cell shortening, which terminates with myxospore production. Under the conditions of our experiments, both myxospore formation and germination (to be de-

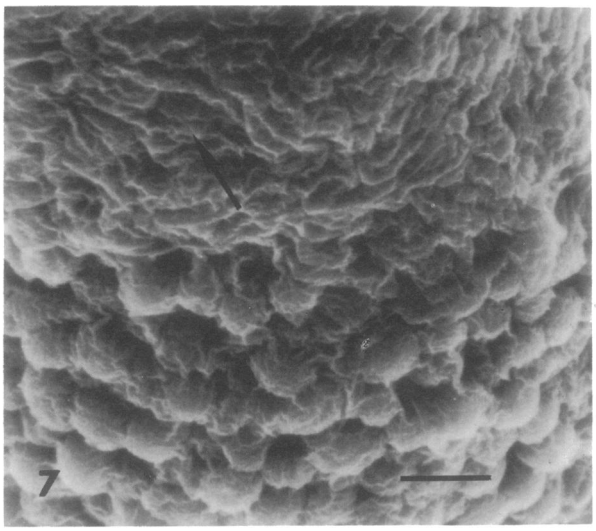

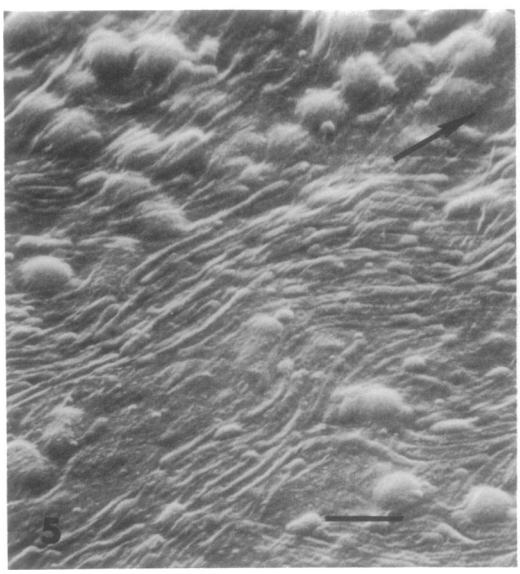

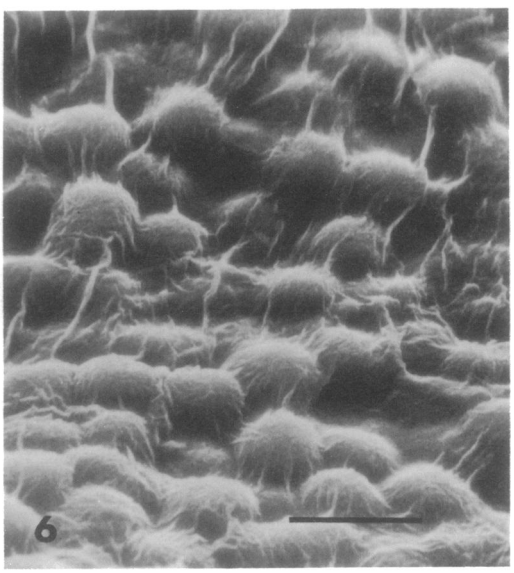

FIG. 5. *Agar surface at the base of a fruiting body of M. xanthus. Arrow indicates direction of base of the fruiting body. Scale marker is 2 μm. 48° tilt.*

FIG. 6. *Myxspores embedded in slime at the basal region of a fruiting body of M. xanthus. Scale marker is 2 μm. 47° tilt.*

FIG. 7. *Slime layer coating myxospores at the apex of M. xanthus fruiting body. Arrow indicates direction of apex. Scale marker is 2 μm. 10 kV; 39° tilt.*

scribed later) in liquid medium were highly synchronous as indicated by the distributions of cell sizes and morphologies. The kinetics of shape change during the morphogenetic process was determined by direct measurement of cell dimensions at various times after induction (Fig. 13). A typical vegetative cell (Fig. 8) has dimensions of 0.75 by 5.2 μm; the range of lengths varied from 3.0 to 7.5 μm. Vegetative cells did not fix well, presumably because the cell wall is discontinuous (20). Thirty minutes after the induction of myxospore formation by glycerol, the longer vegetative cells appeared to have shortened. Little shape change then occurred under our conditions until approximately 75 min, when further shortening to ovoid began (Fig. 9 to 11). Rapid contraction progressed until the unornamented spherical myxospore (average diameter, about 1.2 μm) was formed (Fig. 12). Throughout this shortening

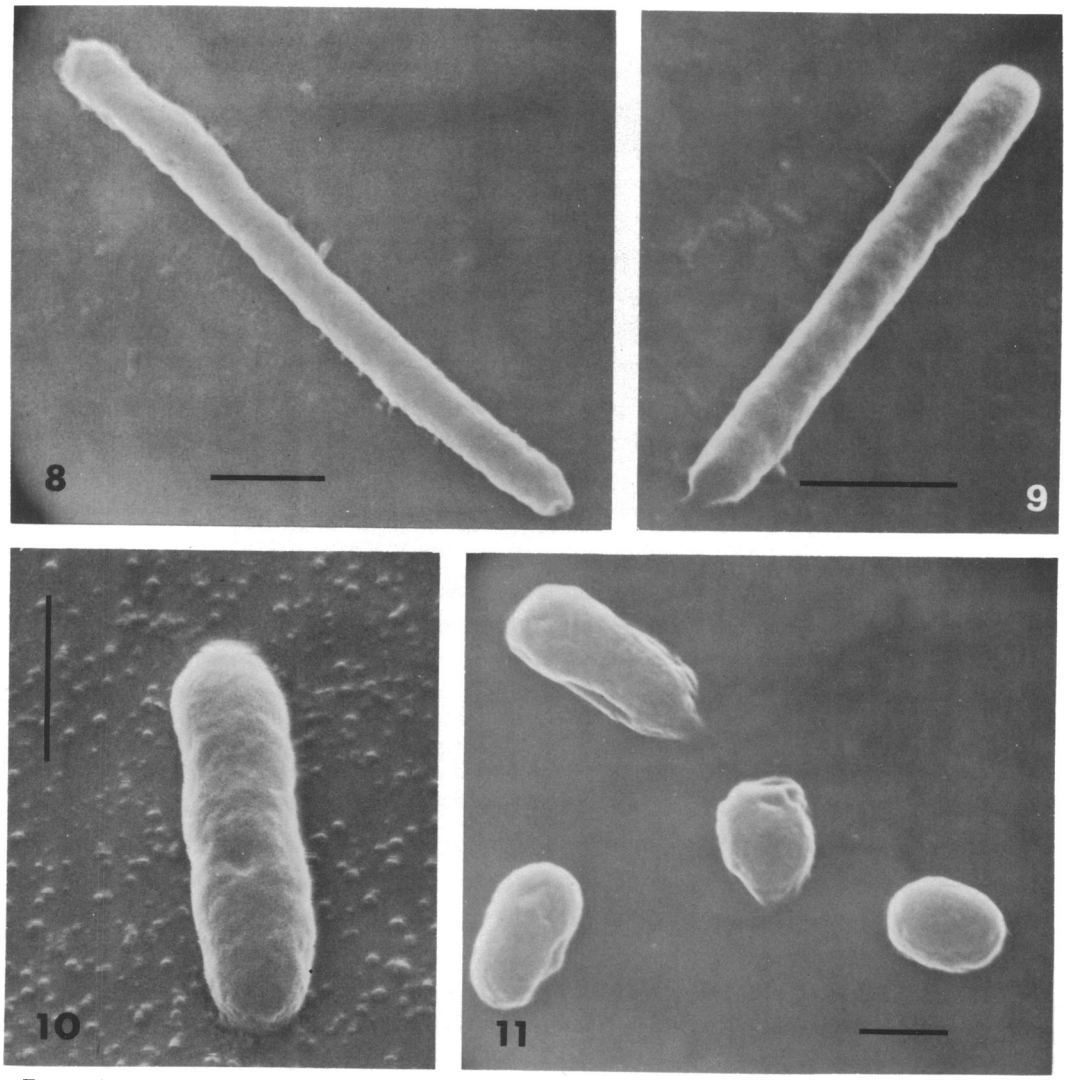

FIG. 8. *Vegetative cell from exponential phase culture of M. xanthus. Scale marker is 1 μm. 0° tilt.*

FIG. 9–11. *Shortening of M. xanthus vegetative rods during glycerol-induced myxospore formation. Scale marker is 1 μm. (Fig. 9). 60 min after induction; 40° tilt. (Fig. 10). 90 min after induction; 20° tilt. (Fig. 11). 105 min after induction; ovoid formation sequence; 15° tilt.*

process the cell surface remained smooth and there was no indication of any surface alteration.

Myxospore germination and cell outgrowth (Fig. 14–20) occurred synchronously when glycerol-induced cysts were resuspended in fresh liquid Casitone medium (see Fig. 13). Shortly after being placed in this medium, the myxospores became somewhat more ovoid and the vegetative cell emerged through one end of the spore wall (Fig. 14). When myxospores differentiated in fruiting bodies on solid medium were examined under these conditions, not only was their germination protracted and asynchronous, but also the myxospore wall or capsule was left behind by the emerging vegetative cell (Fig. 15). This was never observed in the germination of glycerol-induced myxospores. By 45 min, the vegetative cells from glycerol-induced myxospores had further elongated and often showed a pleated appearance (Fig. 16). The spore coat appeared simply to fuse with the wall of the growing vegetative cell (Fig. 16, 17). By 60 min, the emerging cells had lost their smooth surfaces, and little indication of the earlier location of the spore wall remained (Fig. 17). As the vegetative cell enlarged, its surface became severely distorted, with knob-

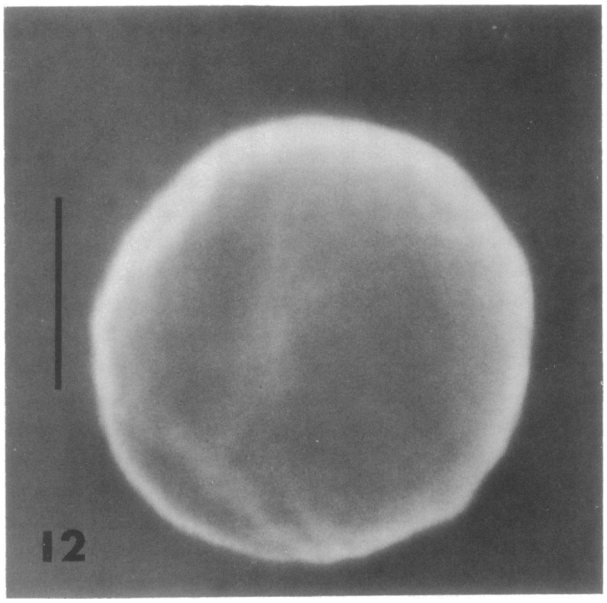

FIG. 12. *Mature glycerol-induced myxospore of M. xanthus. Scale marker is 0.5 μm (original magnification, × 50,000). 15° tilt.*

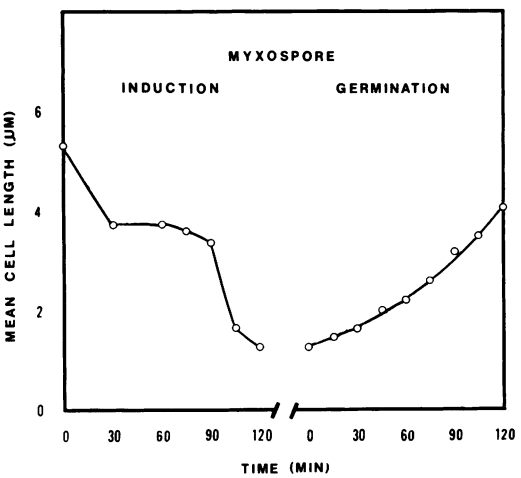

FIG. 13. *Time course of morphological alterations in encysting vegetative cells and germinating myxospores of M. xanthus. Mean cell lengths were determined by direct measurement of 20 cells in an electron micrograph of a representative field for each time point.*

like protuberances and bulges appearing along the length at rather regular intervals (Fig. 18, 19). These persisted throughout the first synchronous cell division (Fig. 20), which occurred 7 h after transfer of myxospores to fresh medium. The cells subsequently assumed the normal appearance of vegetative cells (Fig. 8). In contrast to this, vegetative cells emerging from the capsules of fruiting-body-formed myxospores were long and straight, in every manner identical to exponentially growing vegetative cells.

DISCUSSION

The morphogenetic events comprising the *Myxococcus* life cycle may be thought to begin with the coordinated movement of vegetative cells before fruiting-body formation. Both the mechanism by which this organism effects gliding motility itself and the mechanism by which alignment of migrating cells is coordinated during fruiting-body formation are enigmatic. Our scanning electron micrographs of material fixed in several ways clearly show that no appendages are attached to the cell wall nor is it likely that pores exist through which slime could be excreted to provide a means of propulsion. Freeze-etch and thin-section TEM studies also reveal no surface organs of motility (4, 18). Furthermore, no ultrastructural differences were observed when motile and immotile strains of *M. xanthus* were compared (5). McCurdy has suggested that slime track deposition may play a role in oriented cell streaming during fruiting-body formation in *Chondromyces* (12). We attempted to detect slime tracks formed by aggregating cells on agar surfaces but could not.

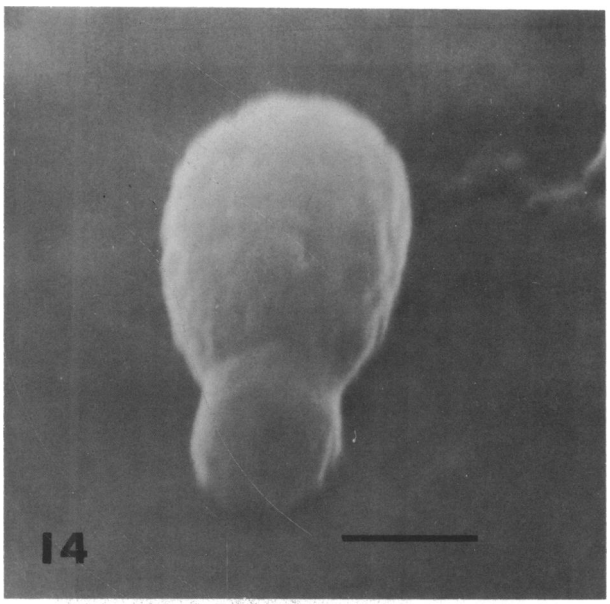

FIG. 14. *Germinating glycerol-induced myxospore (m) showing outgrowth of vegetative cell (v). Germination time (t) is 30 min. Scale marker is 0.5 μm. 45° tilt.*

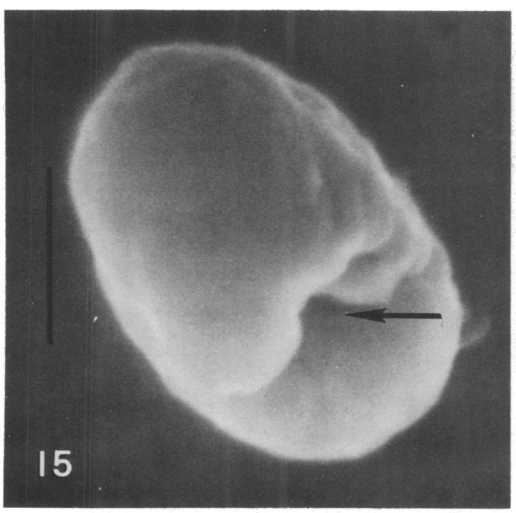

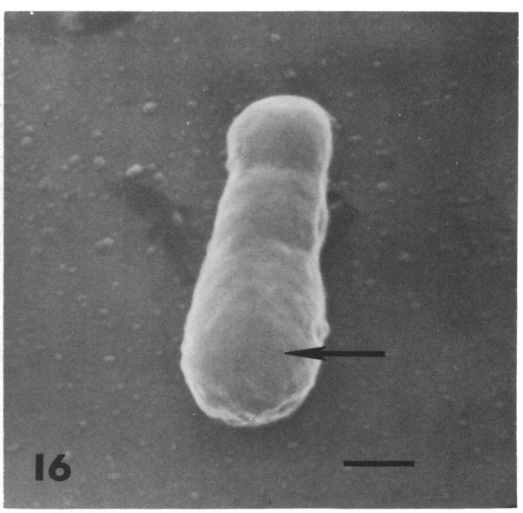

FIG. 15. *Empty spore coat of M. xanthus after germination of myxospore formed in fruiting body (on solid medium). Arrow indicates site of vegetative cell rupture of myxospore wall during outgrowth. Scale marker is 0.5 μm (original magnification, × 50,000). 40° tilt.*

FIG. 16. *Outgrowing vegetative cell of M. xanthus; t = 45 min. Arrow indicates region of original myxospore. Scale marker is 0.5 μm. 28° tilt.*

Thus, the means of movement of *M. xanthus* remains unknown.

The aggregation and differentiation of swarming cells appear to be controlled by a chemotactic response that is under nutritional control (6, 7, 10, 14). The chemotactic substance(s) is as yet unidentified. However, the aggregation of *Myxococcus* cells is reminiscent of the cyclic adenosine 3′,5′-monophosphate-mediated aggregation that occurs in the cellular slime mold *Dictyostelium discoideum* (11). At the foci of aggregation, *Myxococcus* cells form pyramids composed of concentric layers. These cells are cemented together with a thick slime

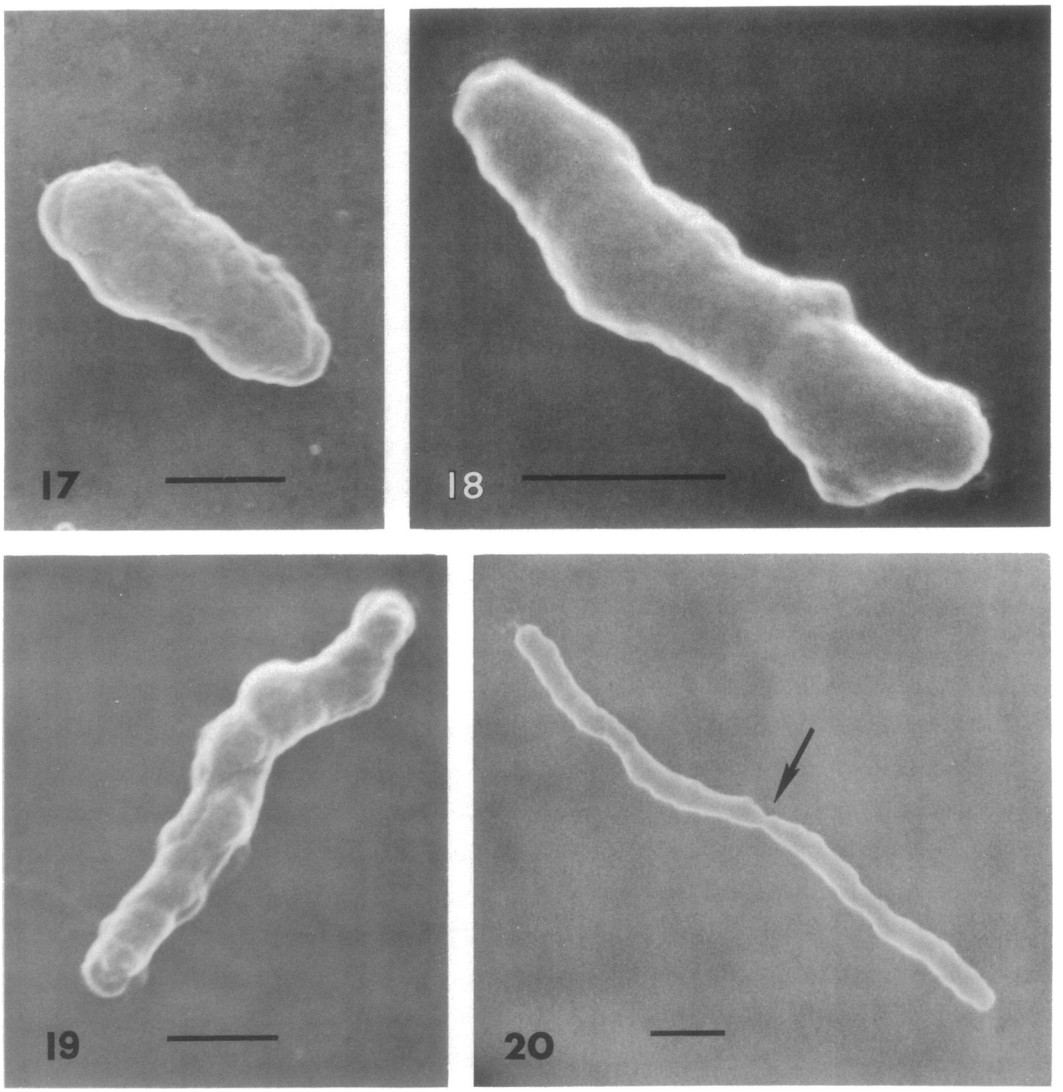

FIG. 17–20. *Later sequential stages in outgrowth of vegetative cells from myxospores of M. xanthus. (Fig. 17). t = 60 min; 0° tilt. (Fig. 18). t = 90 min; 0° tilt. (Fig. 19). t = 120 min; 15° tilt; 25 kV. (Fig. 20). Vegetative cells in first synchronous division completing septation 7 h after germination. Arrow indicates septum formation; 0° tilt. Scale marker is 1 μm.*

layer to form the fruiting body in which all of the vegetative cells are subsequently converted to myxospores. The general appearance of the fruiting body is somewhat variable and seems to depend upon both the number of cells that compose it and the spatial orientation of cell streams that lead to its formation. A comparison of the *M. xanthus* fruiting body to the more complex fruiting structures of other myxobacteria can be had by referring to the scanning electron micrographs of Brockman and Todd (3) and McNeil and Skerman (13).

Myxospores may be formed "naturally" in fruiting bodies on solid agar upon nutritional deprivation (6) or upon induction of liquid cultures by glycerol addition (8). We have noted a number of differences in myxospore formation under these two conditions. It is difficult to directly compare the time course of myxospore formation in these two circumstances because the glycerol induction technique bypasses many of the complex events necessary for fruiting-body formation. Under our conditions glycerol-induced morphogenesis was completed in 2 h, whereas 6 to 9 days were required for myxospore formation in fruiting bodies. We observed that

fruiting-body myxospores were larger (about 2 μm) than glycerol-induced myxospores (about 1.2 μm). This size difference appeared to be due to a thickened slime capsule surrounding the myxospore. The TEM studies of myxospore formation by Voelz and Dworkin (18), when compared with that of Bacon and Eiserling (1), show a considerable difference in the thickness of the capsule layer depending upon the method of myxospore formation.

The kinetics of myxospore germination and vegetative cell outgrowth differ markedly depending upon the conditions of their formation. Under comparable germination conditions, glycerol-induced myxospores germinate rapidly and synchronously; fruiting-body myxospores germinate asynchronously, and the time required is several times that of glycerol-induced myxospores. Such differences might be due to alterations in endogenous pools (e.g., amino acids, nucleotides) since induction in liquid is performed in a rich medium, whereas fruiting-body formation takes place under starvation conditions. Additionally, TEM analysis suggests that glycerol-induced myxospores, in contrast to fruiting-body myxospores, contain vesicles localized between the capsule wall and the cell wall (1). Perhaps these have some role in germination. Outgrowing vegetative cells from fruiting-body myxospores emerge through one region of the elongated spore and shed the capsule wall as shown by us and earlier by Voelz and Dworkin (18). This capsule persists and can be seen at the light-microscope level. However, we never observed empty capsules from glycerol-induced myxospores. Our micrographs suggest in this case that the capsule wall is maintained as part of the emerging vegetative cell. It either fuses with the cell wall or slowly disintegrates.

Finally, there is a marked difference in the appearance of newly emerged vegetative cells. Those derived from fruiting-body myxospores resemble typical exponential vegetative rods as they enlarge to characteristic size. In contrast, the surface of an emerging vegetative cell from a glycerol-induced myxospore initially is smooth, but upon further elongation its shape becomes distorted, with knoblike protuberances. Since this can be seen at the light-microscope level in unfixed, living material as well, it is not an artifact of fixation. This unusual surface structure persists through the first cell division. Reichenbach et al. (15) and Voelz and Reichenbach (19) have shown that in the myxobacterium *Stigmatella*, myxospores derived from cysts had less infolding of cell walls than did those of glycerol-induced myxospores. They suggested that as the surface area of vegetative cells decreases during myxospore formation, the wall material is "folded up" to be reutilized upon cell expansion. Differences in the timing or regulation of cyst-formed myxospores might account for less infolding. Since White et al. (20) have suggested that the murein layer of the *Myxococcus* cell wall is discontinuous, long-lasting effects on cell surface structure as a consequence of murein discontinuities might be expected when cells emerge from glycerol-induced myxospores. The regularly spaced constrictions seen on the irregular surface of cells derived from glycerol-induced myxospores might indicate regions of discontinuity in the cell wall.

ACKNOWLEDGMENTS

We thank W. Miller for excellent technical assistance with the microscopy and M. Dworkin for his gift of the FB strain of *Myxococcus xanthus*.

LITERATURE CITED

1. Bacon, K., and F. A. Eiserling. 1968. A unique structure in microcysts of *Myxococcus xanthus*. J. Ultrastruct. Res. **21**:378–382.
2. Bacon, K., and E. Rosenberg. 1967. Ribonucleic acid synthesis during morphogenesis in *Myxococcus xanthus*. J. Bacteriol. **94**:1883–1889.
3. Brockman, E. R., and R. L. Todd. 1974. Fruiting myxobacteria as viewed with a scanning electron microscope. Int. J. Syst. Bacteriol. **24**:118–124.
4. Buchard, R. P. 1970. Gliding motility mutants of *Myxococcus xanthus*. J. Bacteriol. **104**:940–947.
5. Buchard, R. P., and D. T. Brown. 1973. Surface structure of gliding bacteria after freeze-etching. J. Bacteriol. **114**:1351–1355.
6. Dworkin, M. 1963. Nutritional regulation of morphogenesis in *Myxococcus xanthus*. J. Bacteriol. **86**:67–72.
7. Dworkin, M. 1973. Cell-cell interactions in the myxobacteria in microbial differentiation, p. 125–142. *In* J. M. Ashworth and J. E. Smith (ed.), 23rd Symp. Soc. Gen. Microbiol. Cambridge University Press, Cambridge.
8. Dworkin, M., and S. M. Gibson. 1964. A system for studying microbial morphogenesis:rapid formation of microcysts in *Myxococcus xanthus*. Science **146**:243–244.
9. Hanson, C. W., and M. Dworkin. 1974. Intracellular and extracellular nucleotides and related compounds during the development of *Myxococcus xanthus*. J. Bacteriol. **118**:486–496.
10. Hemphill, H. E., and S. A. Zahler. 1968. Nutritional induction and suppression of fruiting in *Myxococcus xanthus*. J. Bacteriol. **95**:1018–1023.
11. Konijn, T. M., J. G. C. Van de Meene, J. T. Bonner, and D. S. Barkley. 1967. The acrasin activity of adenosine-3′,5′-cyclic phosphate. Proc. Nat. Acad. Sci. U.S.A. **58**:1152–1154.
12. McCurdy, H. D., Jr. 1969. Light and electron microscope studies on the fruiting bodies of *Chondromyces crocatus*. Arch. Mikrobiol. **65**:380–390.
13. McNeil, K. E., and V. B. D. Skerman. 1972. Examination of myxobacteria by scanning electron microscopy. Int. J. Syst. Bacteriol. **22**:243–250.
14. Quinlan, M. S., and K. B. Raper. 1965. Development of the myxobacteria, p. 596–611. *In* W. Ruhland (ed.), Handbuch der Pflanzenphysiologie. Springer-Verlag, Berlin.

15. Reichenbach, H., H. Voelz, and M. Dworkin. 1969. Structural changes in *Stigmatella aurantiaca* during myxospore induction. J. Bacteriol. **97**:905–911.
16. Sadler, W., and M. Dworkin. 1966. Induction of cellular morphogenesis in *Myxococcus xanthus*. II. Macromolecular synthesis and the mechanism of inducer action. J. Bacteriol. **91**:1520–1525.
17. Voelz, H. 1966. The fate of the cell envelopes of *Myxococcus xanthus* during microcyst germination. Arch. Mikrobiol. **55**:110–115.
18. Voelz, H., and M. Dworkin. 1962. Fine structure of *Myxococcus xanthus* morphogenesis. J. Bacteriol. **84**:943–952.
19. Voelz, H., and H. Reichenhach. 1969. Fine structure of fruiting bodies of *Stigmatella aurantiaca* (*Myxobacterales*). J. Bacteriol. **99**:956–866.
20. White, D., M. Dworkin, and D. J. Tipper. 1968. Peptidoglycan of *Myxococcus xanthus*: structure and relation to morphogenesis. J. Bacteriol. **95**:2186–2197.
21. Witkin, S. S., and E. Rosenberg. 1970. Induction of morphogenesis by methionine starvation in *Myxococcus xanthus*: polyamine control. J. Bacteriol. **103**:641–649.
22. Zusman, D., P. Gottlieb, and E. Rosenberg. 1971. Division cycle of *Myxococcus xanthus*. iii. Kinetics of cell growth and protein synthesis. J. Bacteriol. **105**:811–819.
23. Zusman, D., and E. Rosenberg. 1968. Deoxyribonucleic acid synthesis during microcyst germination in *Myxococcus xanthus*. J. Bacteriol. **96**:971–986.